



Automated Classification of Lung Nodules and Precise Segmentation with Convolutional Neural Networks

Ahmed Nidhal Khdiar¹ and Enas Hamood Al-Saadi²

¹Department of Electrical engineering, Faculty of Engineering, University of Kufa, Najaf, Iraq

²Department of Computer, College of Education for Pure Science, University of Babylon, Babylon, Iraq

E-mail address: ahmed.elabadi@uokufa.edu.iq, pure.anas.ehmod@uobabylon.edu.iq

Received ## Mon. 20##, Revised ## Mon. 20##, Accepted ## Mon. 20##, Published ## Mon. 20##

Abstract: Among the deadliest cancers, lung cancer is very deadly, frequently having fatal results. Medical professionals face complex challenges when using CT scan pictures to assess cancer. As a result, there is an urgent need to create computer-aided systems that may reduce processing time and human labor while simultaneously properly detecting and classifying lung cancer. This research proposal is dedicated to the pivotal task of lung nodule detection, classification into benign or malignant categories in early cancer diagnosis, and subsequent precise segmentation of lung cancer nodules, offering insight into their spatial extent within the CT images based on robust deep learning network. Extensive parameter optimization has been undertaken to craft an efficient and powerful convolutional neural network (CNN) architecture. One of the standout features of this research is its ability to not only accurately classify lung nodules but also precisely delineate their spatial boundaries, calculate their areas, and pinpoint their exact locations within medical images. Our approach leverages a bespoke convolutional neural network (CNN) architecture, meticulously fine-tuned through empirical experimentation, to achieve a remarkable accuracy rate of 99.17%, precision rate of 99.01%, recall rate of 99.75%, and F1-score rate of 99.37%. This surpasses the performance of existing methods in the field and marks a significant breakthrough in lung cancer detection and analysis. The results offer a promising step forward in early diagnosis and treatment planning for lung cancer patients, ultimately contributing to enhanced patient care and outcomes.

Keywords: Computer-aided diagnosis, Early cancer detection, Image analysis, Medical image, Radiology.

1. INTRODUCTION

Cancer, a collective term for a group of diseases, is marked by irregular cell growth and reproduction, leading to the destruction of healthy cells in the body. These cancerous cells possess the capacity to multiply and metastasize, spreading from one organ to another within the human body. Fig. 1 illustrates the most prevalent types of cancer [1].

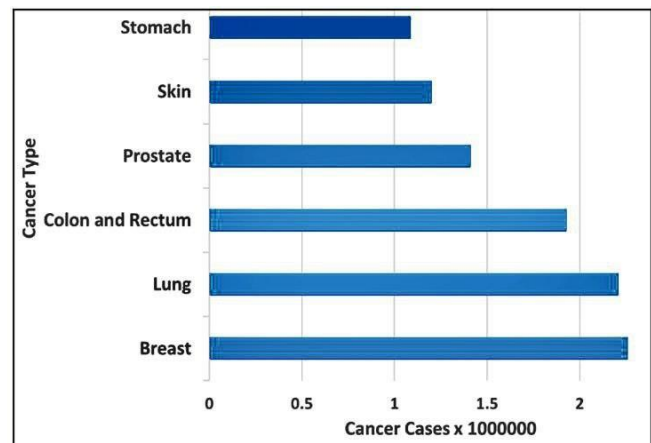


Figure 1. The number of cancer cases for the most public cancer type [1].

Fig. 2 shows that lung cancer is the type of cancer that kills people the most frequently worldwide. Cancer mortality is reduced when cases are detected and treated early [2].

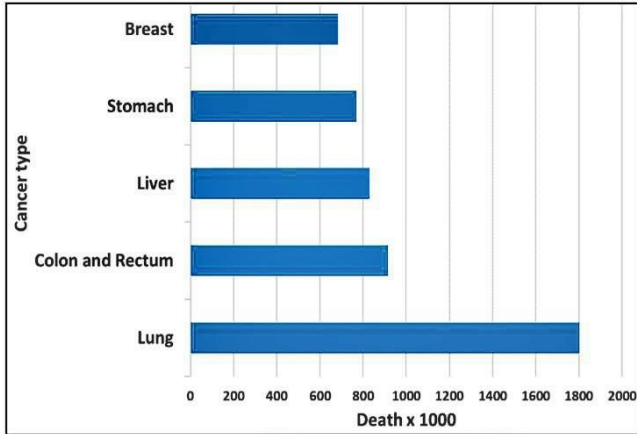


Figure 2. The number of deaths for the most public cancer type [1].

The American Cancer Society states that lung cancer is the primary cause of cancer-related mortality. According to cancer statistics from 2022, there were 609,360 cancer-related fatalities and nearly 1.9 million recorded illnesses. Lung cancer was the cause of nearly 350 of these deaths every day. Cancer is still a major health problem despite advancements in medicine, and it is still exceedingly difficult to effectively treat and prevent its various forms. Owing to its variety, cancer therapy is intricate and challenging. Additionally, early detection is crucial because some cancers can be lethal. As screening searches for cancer cells in people who are asymptomatic, it is essential for early cancer detection. In the fight against cancer, this stage is crucial because it enables early discovery, which is necessary for efficient treatment. In order to develop an appropriate treatment plan, medical imaging equipment offer crucial information regarding the kind and stage of cancer. Therefore, in order to diagnose cancer early, it is essential to provide clinical follow-up for patients and to conduct cancer tests. Patient outcomes are improved by this strategy because it makes treatment planning easier. The accuracy of disease diagnosis and treatment outcomes is significantly influenced by the caliber of the data gathered using scanning technology. The total quality and duration of life of patients can be enhanced by precise analysis based on trustworthy screening procedures and treatment plans. The extremely successful treatment plans can only be seen with the use of contemporary cancer imaging equipment. Throughout the difficult treatment procedure, patients who receive the required imaging tests and inspections have a considerable edge over other patients. In order to determine the best treatment strategies and, eventually, enhance patient

outcomes, a thorough examination of imaging data is vital [3].

Detecting lung cancer in its early stages can be a formidable challenge due to the striking morphological similarities between cancerous and noncancerous lung nodules, necessitating discriminatory diagnostics reliant on subtle distinctions in morphology, location, and clinical biomarkers. The identification of malignancy in these nodules during their early development poses a particularly daunting task [4]. This complexity arises from the wide spectrum of nodule sizes, shapes, locations, and densities encountered in clinical practice. Consequently, numerous researchers have endeavored to address this challenge by devising optimal feature sets leveraging advanced image processing techniques.

Traditional computer-aided diagnosis systems relied on manual feature extraction, encompassing aspects like texture and shape analysis. However, these manually derived features are subjective, particularly when dealing with medical images of variable quality. Moreover, their abstract nature can limit their utility. Additionally, It takes a long time to manually extract features, lacks uniformity, and is prone to issues related to normalization and universality.

Crucially, the key to improving patients' survival rates lies in early detection. As a result, there has been an increasing demand for computer-aided systems that enable early and precise lung cancer detection [2].

The subsequent sections of this paper are structured as follows: In addition to this introduction, The contributions are introduced in section two. An overview of relevant works is given in section 3, and the dataset is described in section 4. In section 5, the convolutional neural network is the primary subject. Section sixth delves into the methodology employed. The seventh section include the paper's result, discussion and evaluation measures of our research, respectively. Finally, Section eight encapsulates our findings and conclusions.

2. The Contributions

1. One CT lung picture prediction using the recommended diagnosis approach takes only 0.06 seconds.
2. Unlike the most recent models, the system predicts rapidly and with fewer parameters, allowing it to be employed in real-time.
3. For disease diagnosis, the proposed technique produced superior outcomes in terms of classification system accuracy as compared to earlier researchers.

3. Literature Review

Mask Region Convolutional Neural Network (Mask-RCNN) and Dual Path Network (DPN) algorithms were integrated as recommended by (J. Feng and J. Jiang, 2022) for segment lung cancer patient's CT scans and pulmonary nodules' enhanced CT images were looked at and studied.

It is important to recognize certain study limitations. The study's power was diminished due to the limited sample size. An increased sample size in the follow-up is required to support the study's conclusions. There are many potential clinical applications for the integration of medical imaging technology and artificial intelligence algorithms, making this combination worthy of clinical advancement. Combining deep learning-based CT using serum tumor marker data increased accuracy up to a certain point, 97.94%. up to a certain point, 97.94% [5].

Computed tomography (CT Scans) was utilized by (R. Bhalerao et al.,2019) to identify and categorize the lung nodules. An image in grayscale is created from the input color image and then converted into a binary image. These images were used for training the convolutional neural network on the classification of the lung nodules as benign or malignant. The suggested article demonstrates the entire image processing process, beginning with the extraction of image data from several sources such as LIDC, LUNA16, and Kaggle. Because the CNN method produces better results than machine learning designs like SVM and Naïve Bayes, it was chosen. The accuracy was about 94.46% [6].

(J. Soltani-Nabipour et al., 2020) presented an improved region-growing (IRG) method for segmented lung tumors. According to previously collected data, IRG algorithm stages were limiting the growth region. Automatic threshold detection and step-by-step comparative value updating, growing from a few points, and Edge correction. Overall, it was found in this study that the algorithm's use had little impact on the outcomes obtained and improved tumor identification by less than 13%. Its accuracy was 98% [7].

(M. Rehman et al.,2020) used the Japanese Radiological Technology Society (JSRT) dataset to classify 247 three-dimensional images. The images were preprocessed and converted to grayscale. The model for detecting lung cancer was developed through the use of a Convolutional Neural Network. Comparing the model to other classification methods, the model had the lowest accuracy and the highest loss rate. The accuracy achieved by this model was 88 % [8].

A method that consists of two phases, the first of which is the multi-planar nodule identification and the second of which is the false-positive decrease, was developed by (S. Zheng et al., 2021). The initial step involved finding potential nodule candidates on the axial, coronal, and sagittal planes using the convolution neural network model U-net++. To successfully eliminate false positives, multi-scale, dense convolution neural networks are used in the second stage. This system's inability to recognize tiny nodules was a problem. Convolutional neural networks performed better when multiscale features were shared. The designed system achieves 94.6 % sensitivity for small nodules [9].

4. Dataset Used

In this proposal, the (TCIA) Lung CT Challenge dataset was used [10]. The images in the dataset are labeled as benign and malignant. Also, the nodule is bounded which gives a good opportunity to measure the performance of the suggested segmentation method. For each patient, there is a set of images of the lung that were taken from different directions and angles. This dataset contains 11,114 labeled CT lung images, Images of 8286 malignant tumors, and 2828 benign nodules. Fig. 3 shows a sample of images from the dataset.

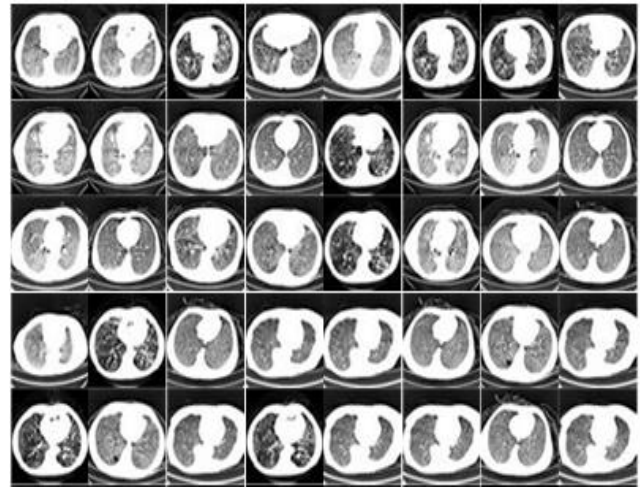


Figure 3. Sample of images from the SPIE-AAPM dataset

5. Convolution Neural Network

A CNN is made up of a stack of layers, including convolutional, pooling, rectification, fully connected (FC), and loss layers. The incoming data is transformed by these layers into extremely nonlinear representations. The convolution process is performed on the input image or the features map (input from the previous layer) with filters, it is used to extract the features. Generally, low-level features are extracted in the first layer, and each of the next layers extracts features more complex than the previous.

The optimal size of the input image is (50x50). In this proposal, a filter size of (7x7) with 64 filters in the first layer was used, and 32 filters for the second layer. The classification results are the results for the fully connected layer which is the final layer. The final layer used the Sigmoid classification tool to categorize the image as benign or malignant. This network makes use of the Adam optimizer. Fig. 4 depicts the suggested CNN architecture.

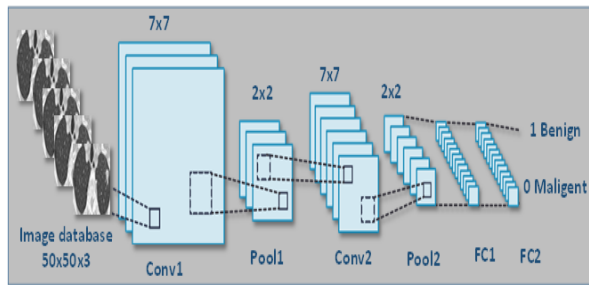


Figure 4. The proposed CNN Architecture.

6. Proposed Method

The aim of this proposal is the detection, classification, and localization of lung nodules in CT images. Using the Convolutional Neural Network (CNN) for this purpose was suggested. The proposed CNN is designed to be appropriate for lung nodules classification and most of the important optimal CNN parameters are determined. To achieve the aim of this proposal, the network was trained on the benign and malignant lung images, and then the network for a test with different images. Fig. 5 depict the block diagrams for the proposed model.

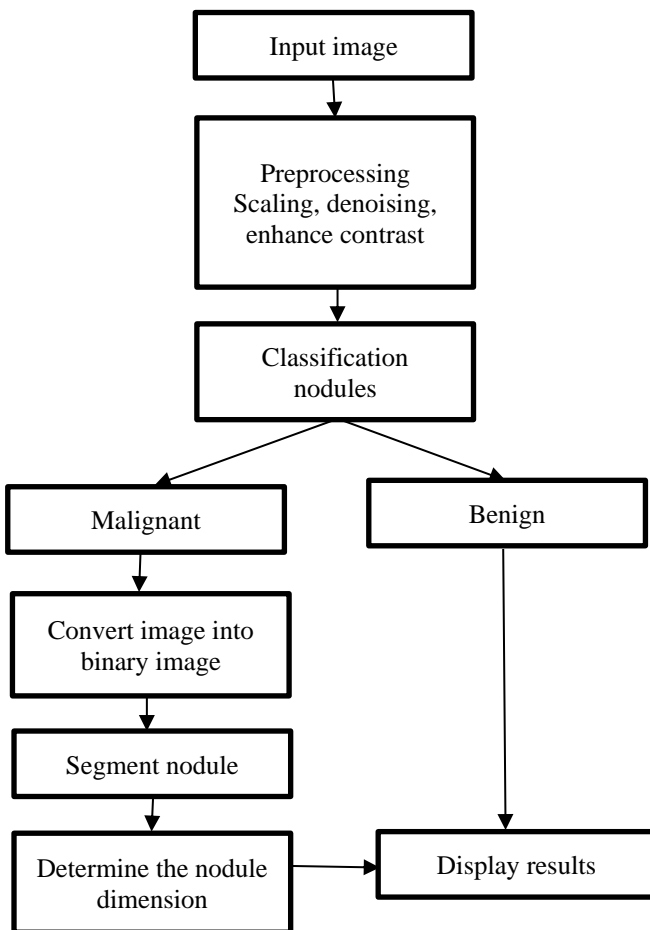


Figure 5. Block diagram of the proposed model

A. Preprocessing

The first step in this stage is scaling down the images to (50×50) pixels, which is appropriate for CNN. The next step in this stage is denoising, salt and paper noise almost contaminate the lung images. Fig. 6 shows the efficiency of a median filter.

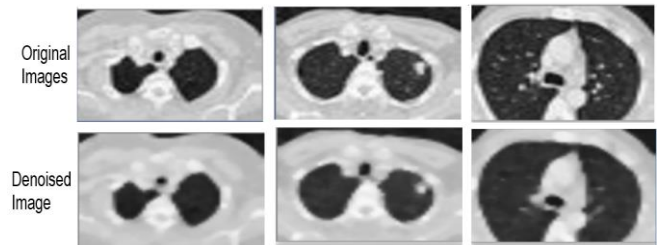


Figure 6. The denoising of the lung images.

The final step is the image contrast enhancement based on gamma correction. The value of gamma has a high effect on image enhancement, so many values of gamma (chosen by experimentation) were tested until the best value of gamma was obtained. The contrast step is the crucial step that affects the next steps and the segmentation of nodules. Using the incorrect value of gamma will lead to inaccurate segmentation. A sample of the effect of using a high value of gamma on input images is shown in Fig. 7 in this case the nodule becomes almost similar to the background and then which causes the nodule and gives another region that is not related to the actual.

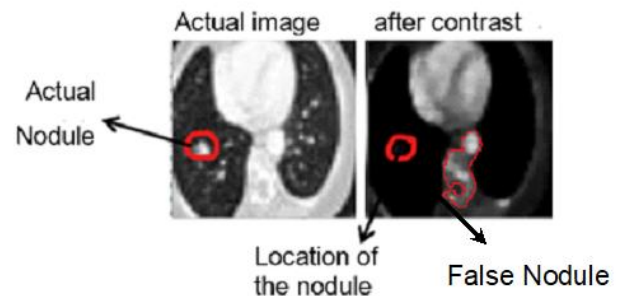


Figure 7. The results of segmentation when using gamma value equal seven.

On the other side, when the gamma is small (in this sample gamma equals 0.1), in this case, maybe more than one region is obtained as a nodule, hence it is very difficult to recognize the actual nodule as shown in Fig. 8.

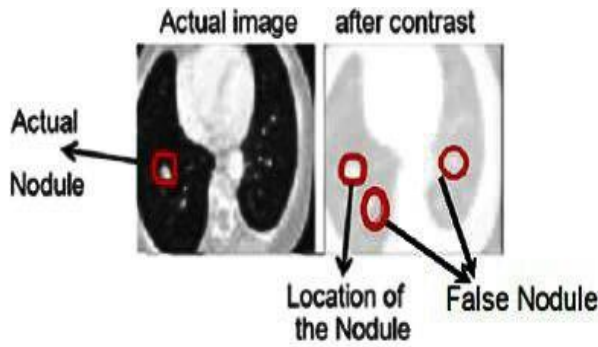


Figure 8. Using small gamma which leads to confusion of nodules.

The gamma value was measured experimentally and the optimum value for enhancing the contrast is equal to 1.2, as shown in Fig. 9.

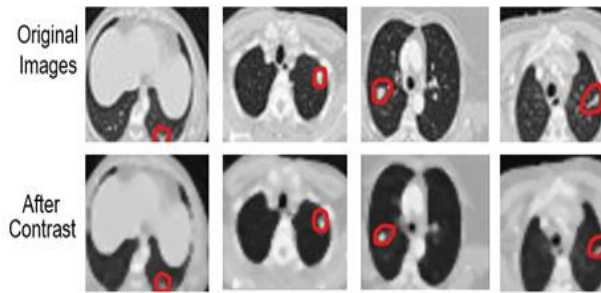


Figure 9. The results of segmentation when using gamma value equal 1.2.

B. Proposed Convolution Neural Network

In the current proposal, the preprocessing input lung image to the suggested CNN is classified into two categories (benign or malignant). A sample of these images is shown in Fig.10.

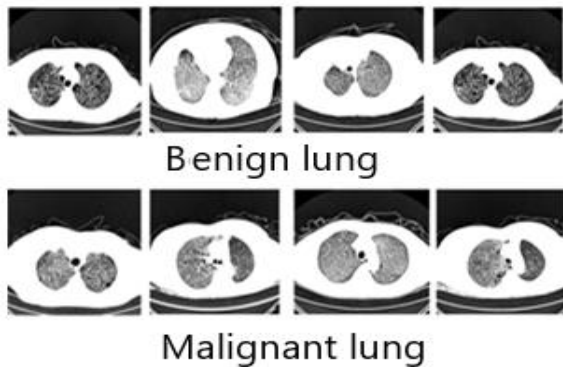


Figure 10. Sample of benign and malignant images.

Two (convolution layers, max-pooling, and entirely connected layers) make up the proposed CNN architecture. The details of the proposed CNN layers and their parameters are shown in Table I.

TABLE I. THE DETAILS OF THE PROPOSED MODEL

Layer (Type)	Output Shape	Param #
conv2d (Conv2D)	(None, 44, 44, 64)	9472
activation (Activation)	(None, 44, 44, 64)	0
max_pooling2d (Max_pooling2d)	(None, 22, 22, 64)	0
conv2d_1 (Conv2D)	(None, 16, 16, 64)	200768
activation_1 (Activation)	(None, 16, 16, 64)	0
max_pooling2d_1 (Max_pooling2d)	(None, 8, 8, 64)	0
flatten (Flatten)	(None, 4096)	0
dense (Dense)	(None, 64)	202208
activation_2 (Activation)	(None, 64)	0
dense_1 (Dense)	(None, 2)	65
activation_3 (Activation)	(None, 2)	0
Total Params: 472,513		
Trainable params: 472,513		
Non-trainable params: 0		

The CNN uses the Max Pooling layer and numerous convolution layers to identify the key features present in images of the eye fundus, The structure for feature extraction will be like this: The first layer is made up of 64 convolutional filters with a filter size of (7,7) and no padding. Next is the activation function (ReLU), and finally the Max Pooling layer, which has a filter size of (2,2) and strides of (2,2). We then employ further convolution layers (the second convolutional layer has 64 filters), with the filter sizes for the first and second layers being (7,7), the padding remaining the same, and the (ReLU) activation function coming next. The Max pool layer then follows, with filter sizes of (2,2) and steps of (2,2). The Flatten layer comes next. This layer is going to change the feature matrix map into only one column (vector) of values. Afterwards, there will be a Dense layer with 64 units (the size of the output layer), followed by a Dense layer with two classes (malignant or benign) and Sigmoid as the activation function.

C. Nodules Segmentation

After classifying the nodule as malignant, the malignant nodule was segmented, this process means localizing the nodule which helps the physicians to know exactly the location of the nodule.

First, the gray image is converted into a binary image based on the threshold. The threshold is determined by using the Otsu method (Minimal variation between segments), which is a segmentation method that changes the gray value from greater than the threshold to 255 and from less than the threshold to 0 depending on a region that automatically determines thresholds, the result of this step is shown in Fig. 11.

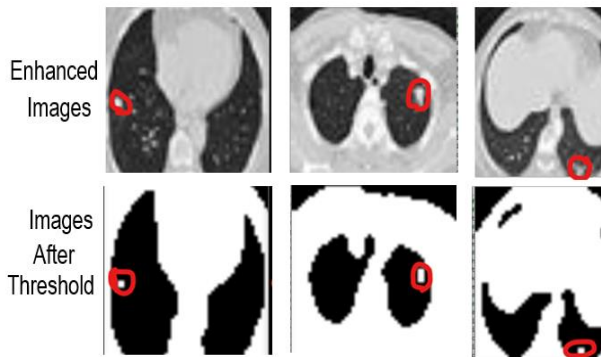
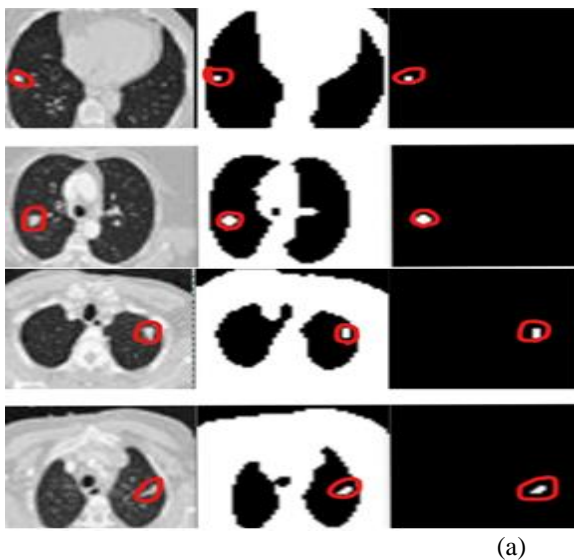


Figure 11. Converting the grayscale images into binary images.

The smallest connected pixel with white color in the binary image is the nodule, so the color of every pixel outside this region is converted into black color when the nodule(s) are isolated, then can be measured in their center and area. Samples of the results from this step are shown in Fig. 12.



(b) (c) (a)
Figure 12. Steps of isolating the nodule: (a) enhanced image, (b) binary image, (c) segmented nodules.

The final step in the segmentation stage is to find the dimensions of the nodules. The area of the nodule is represented by the number of white pixels for the final image. Also, the center of the nodule in the image must be determined, a sample measuring the area and location of a segmented nodule is shown in Fig. 13.

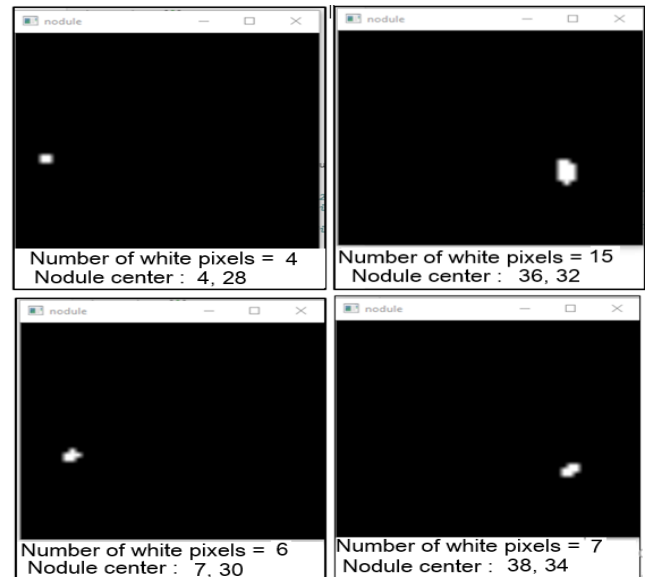


Figure 13. Sample, measuring the area and location of the segmented nodule.

7. Results and Discussion

The proposed method was tested to identify the ideal settings for this algorithm's parameters that improve efficiency, evaluate a network performance for detection and classification, and evaluate the segmentation process.

A. Evaluate the CNN Parameters

In each CNN proposal, various filter sizes and the number of filters have been used. The filter is a window that scans the image to decide the features that belong to each pixel such as an arc, straight line, diagonal, etc. The filter size is related to the number of neighbor information that can be seen when processing the current layer. There is no way to determine the filter size, instead, it is measured experimentally.

The optimum filter size used in the current proposal is measured by testing the performance of the suggested model with various filter sizes as shown in Fig. 14, the best filter size is $(7*7)$ which gives better accuracy.

Also, the number of filters used in this proposal is measured experimentally, by measuring the accuracy of the model with different numbers of filters shown in Fig. 15. When there are 64 and 100 filters, the best performance is obtained. Using 64 filters is preferable to using 100 filters because they could prolong testing.

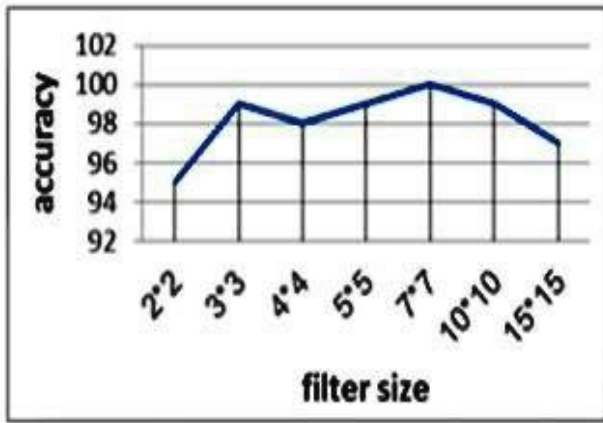


Figure 14. Filter size and network performance relationship.

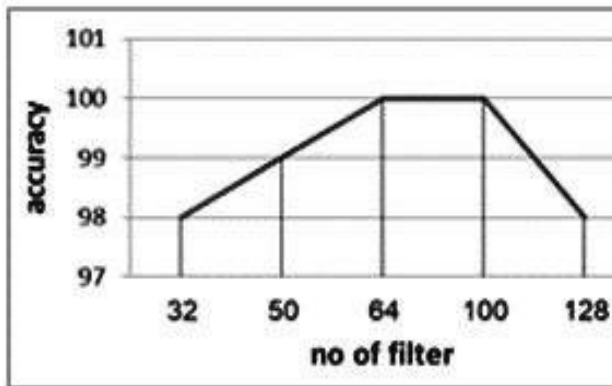


Figure 15. Number of filter and network performance relationships.

Another factor that has a high effect on network efficiency is the number of epochs, which decides how many times the weights of the network must be changed. The neural network's weights change more frequently as the number of epochs increases, as well as the boundary shifts between underfitting, optimum, and overfitting. Different epochs (10, 20, 30, 40, 50, 60, 70, 75, 100, and 200) were used to test the performance of the recommended network. As seen in Fig. 16, 75 epochs was the ideal number.

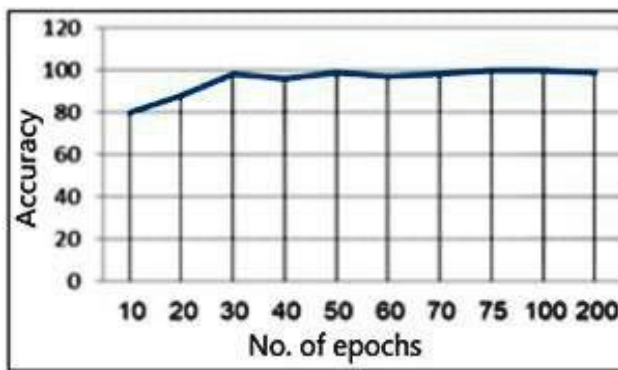


Figure 16. The relationship between the number of epochs and the network accuracy.

Optimizers are ways used to reduce the losses and provide the most accurate results possible, by changing the attributes of the neural network such as weights and learning rate. The recommended network can use a variety of optimizers, including the Adam, Adagrad, Adadelata, and Nadam optimizers. Each of these optimizers is different in terms of performance and benefits. Consequently, the effectiveness of the proposed model is assessed for each of these optimizers, as depicted in Fig. 17. The majority of optimizers affect the suggested network in the same way. As a result, the Adam optimizer is chosen to be used in the present proposal.

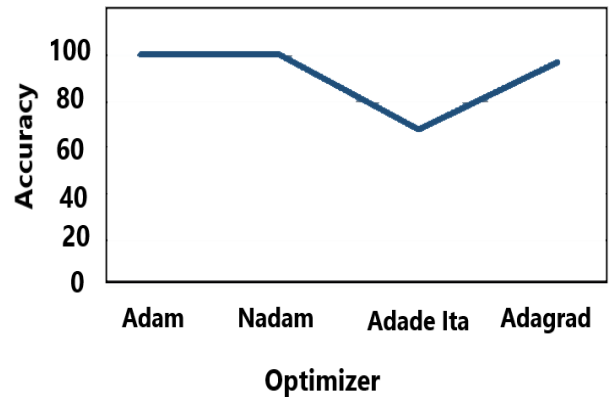


Figure 17. Effect of the optimizer type on the network performance.

In computer vision, the crucial point in the preprocessing stage is image resizing. Principally, using small images in training and testing deep learning is faster, but it needs to be paid attention to because the images might be compressed to the point where important details are lost. For that, the best image size must be determined. The network performance with many image sizes was tested as shown in Fig.18. The test proved that the image size (50x50) of the lung CT image is the optimum size.

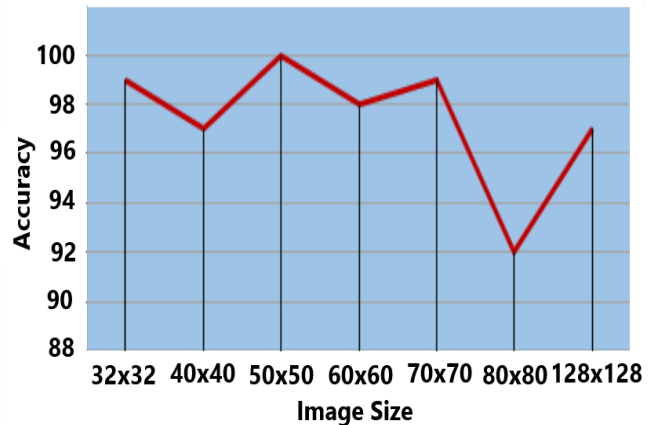


Figure 18. The relationship between image size and network performance.



A summary of the proposed CNN architecture in this section is listed in Table II.

TABLE II. THE ARCHITECTURE OF THE DESIGNED CNN.

Parameter	Description					
Image size	50×50					
Convolution layer	No. of layers	No. of filters	Filter size	Activation function	No. of max-pool	Pooling size
	2	64	7×7	Relu	2	2×2
Fully connected layer	No. of layers		No. of neurons in FCI		Activation Function in FC1 Activation Function in FC2	
	2		64		Relu Sigmoid	
Optimizer	Adam					
Epoch	Epochs No.=75					
Patch	Patch size=64					

B. Evaluate the Model Performance

The suggested model is trained on the many lung images as mentioned previously. The evaluation of the training stage is measured by the system, where the system draws two graphs one for the training accuracy, and the other graph for the loss function, as shown in Fig. 19. The accuracy at the training stage will be best at the number of epoche equal 75, also at this case, the loss is the minimum.

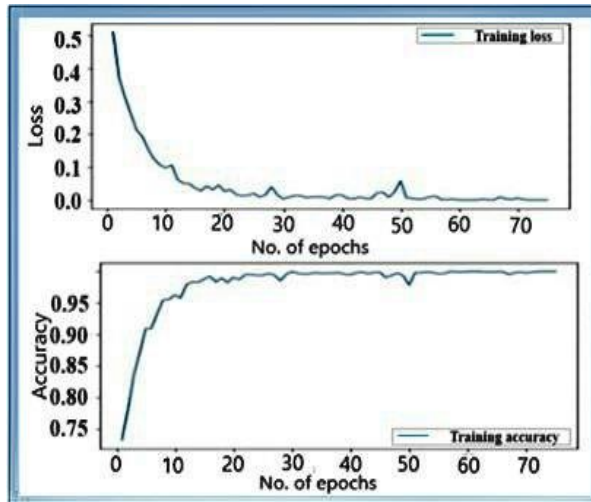


Figure 19. The relationship between the number of epochs and network performance at the training stage.

After the training stage, the model with different data was evaluated. The model was tested with new images that were not used in the training. 606 images for the testing stage were used, where 202 images were benign images and 404 images were malignant images.

Numerous metrics are used to gauge performance, such as:

- Accuracy: If the classification is accurate, success has been achieved regardless of positive or negative classification findings.

$$Acc = \frac{(TP+TN)}{(TP+TN+FP+FN)} \quad (1)$$

- Sensitivity: Is the accurate rate of identifying positive samples.

$$Sen = \frac{TP}{(TP+FN)} \quad (2)$$

- Precision: Assesses the accuracy with which a model predicts positive labels.

$$Pre = \frac{TP}{(TP+FP)} \quad (3)$$

- Recall: Represents the percentage of correctly identified negative cases.

$$Rec = \frac{TP}{(TP+FN)} \quad (4)$$

- F1: Shows how to calculate a balanced mean output by combining sensitivity and accuracy.

$$F1 = 2 \times \frac{Pre \times Rec}{Pre + Rec} \quad (5)$$

There are four parameters that record the prediction error:

- * When the ailment is detected during its manifestation, the test result is considered true positive (TP).
- * When a test result is true negative (TN), it means that the condition was not detected when it was missing.
- * When a test result indicates a condition when it is not present, it is called a false positive (FP).
- * A test result that fails to identify the condition while it is present is known as a false negative (FN).

The proposed model successfully predicts and classifies most of the tested images. The confusion matrix of the testing data and the measurements that can be determined from it (the accuracy, precision, recall, and F1-score) are shown in Fig. 20.

		Prediction	
		malignant	Benign
Actual	malignant	403	1
	Benign	4	198

Accuracy = 99.17
Precision = 99.01
Recall = 99.75
F1 = 99.37

Figure 20. Confusion matrix of the testing proposed model.

As indicated in Table III, the suggested method demonstrated potential and improved lung cancer detection accuracy when compared to previous methods.

TABLE III. COMPARING THE SUGGESTED METHOD WITH PREVIOUS METHODS

Author	Year	Method	Accuracy %
(Q. Song et al., 2017) [11]	2017	CNN	84.2
(S. Hussein et al., 2017) [12]	2017	High-level attributes + CNN	92.3
(A. Nibali et al., 2017) [13]	2017	Rest Net	89.9
(W. Shen et al., 2017) [14]	2017	Multi-crop Convolutional Neural Networks	87.14
(S. Hussein et al., 2017) [15]	2017	3D CNN-Based Multi-task Learning	91.26
(Y. Xie et al., 2017) [16]	2017	Transferable Multi-Model Ensemble	91
(Y. Xie et al., 2018) [17]	2018	Fusing Texture, Shape and Deep Model-Learned Information at Decision Level	88.73
(Y. Xie et al., 2019) [18]	2019	Deep learning	91.6
(G. Zhang et al., 2019) [19]	2019	Hybrid features	93.78
(P. Wu et al., 2020) [20]	2020	Deep residual networks and migration learning	98.23
(G. Shah et al., 2020) [21]	2020	Deep learning	95
(E. Lv et al., 2021) [22]	2021	Deep Convolutional Network	96
(G. Zhang et al., 2021) [23]	2021	3D DenseNet	92.4
(J. Feng and J. Jiang, 2022) [5]	2022	Deep Learning	97.94
P. Bruntha et al., 2022) [24]	2022	Transfer learning	97.93
Proposed model	2023	Deep learning	99.17

8. Conclusion

In the pursuit of predicting, classifying, and precisely segmenting lung cancer nodules, this study has introduced a robust deep-learning network. The proposed neural network has demonstrated exceptional efficacy in discriminating between benign and malignant lung nodules, a crucial step in early cancer diagnosis. A convolutional neural network (CNN) architecture that is both powerful and efficient has been created after extensive parameter optimization. This study's capacity to properly identify lung nodules, define their spatial borders, compute their areas, and locate them exactly inside medical imaging is one of its most notable features. With an outstanding accuracy rate of 99.17%, our approach surpasses the performance of comparable studies, underscoring its potential as a valuable tool in clinical practice. 99.01% precision, 99.75% recall, and an F-score of 99.37% are the outcomes of the design and training for the suggested system, demonstrating the great performance of our model. Furthermore, this work paves the way for future research directions. As a natural progression, it is recommended that future studies extend this framework to encompass the classification of malignant nodules into specific cancer subtypes. Such an advancement holds the promise of further improving cancer diagnosis, treatment planning, and patient care.

REFERENCES

- [1] J. Ferlay, M. Ervik, F. Lam, M. Colombet, L. Mery, and M. Piñeros (2021). Global Cancer Observatory: Cancer Today, International Agency for Research on Cancer (IARC) Working Group, Lyon. <https://gco.iarc.fr/today>
- [2] A. Tiwari, "Prediction of lung cancer using image processing techniques: a review", *Advanced Computational Intelligence: An International Journal (ACII)*, vol. 3, no. 1, pp. 1-9, 2016. <https://airconline.com/acii/V3N1/3116acii01.pdf>
- [3] M. Nair, S. Sandhu, and A. Sharma, "Cancer molecular markers: a guide to cancer detection and management", *Semin Cancer Biol*, vol. 52, pp. 39-55, 2018. <https://doi.org/10.1016/j.semcancer.2018.02.002>
- [4] G. Silvestri, N. Tanner, P. Kearney, A. Vachani, P. Massion, A. Porter, S. Springmeyer, K. Fang, D. Midthun, and P. Mazzone, "Assessment of plasma proteomics biomarker's ability to distinguish benign from malignant lung nodules: results of the PANOPTIC (Pulmonary Nodule Plasma Proteomic Classifier)", *Chest*, vol. 154, no. 3, pp. 491-500, 2018. doi: 10.1016/j.chest.2018.02.012.



- [5] J. Feng, and J. Jiang , “Deep learning-based chest CT image features in the diagnosis of lung cancer”, Computational and Mathematical Methods in Medicine, vol. 2022, pp. 1-7, 2022. <https://doi.org/10.1155/2022/4153211>
- [6] R. Bhalerao, H. Jani, R. Gaitonde, and V. Raut, “A novel approach for detection of lung cancer using digital image processing and convolution neural networks”, In 5th International Conference on Advanced Computing & Communication Systems (ICACCS), 2019, pp. 577-583. <https://ieeexplore.ieee.org/document/8728348>
- [7] J. Soltani-Nabipour, A. Khorshidi, and B. Noorian, “Lung tumor segmentation using improved region growing algorithm”, Nuclear Engineering And Technology, vol. 52, no. 10, pp. 2313-2319, 2020. <https://doi.org/10.1016/j.net.2020.03.011>
- [8] M. Rehman, N. Nawi , A. Tanveer , H. Zafar, H. Munir, S. Hassan, “Lungs cancer nodules detection from CT scan images with convolutional neural networks”, In International Conference on Soft Computing and Data Mining, Recent Advances on Soft Computing and Data Mining, 2020, pp. 382-391. https://link.springer.com/chapter/10.1007/978-3-030-36056-6_36
- [9] S. Zheng, L. Cornelissen, X. Cui, X. Jing, R. Veldhuis, M. Oudkerk, and P. Ooijen, “Deep convolutional neural networks for multiplanar lung nodule detection: improvement in small nodule identification”, Medical Physics, vol. 48, no. 2, pp. 733-744, 2021. [doi:10.1002/mp.14648](https://doi.org/10.1002/mp.14648)
- [10] K. Clark, B. Vendt, K. Smith, J. Freymann, J. Kirby, P. Koppel, S. Moore, S. Phillips, D. Maffitt, M. Pringle, L. Tarbox, and F. Prior , “The cancer imaging archive (TCIA): maintaining and operating a public information repository”, Journal of Digital Imaging, vol. 26, no. 6, pp. 1045-1057, 2013. [doi: 10.1007/s10278-013-9622-7](https://doi.org/10.1007/s10278-013-9622-7)
- [11] Q. Song, L. Zhao, X. Luo, and X. Dou, “Using deep learning for classification of lung nodules on computed tomography images”, Journal of Healthcare Engineering, vol. 2017, pp. 1-7, 2017. <https://doi.org/10.1155/2017/8314740>
- [12] S. Hussein , R. Gillies, K. Cao, Q. Song, & U. Bagci, “Tumornet: lung nodule characterization using a multi-view convolutional neural network with Gaussian process”, IEEE International Symposium on Biomedical Imaging, vol. 2017, pp. 1007-1010, 2007. <https://arxiv.org/abs/1703.00645>
- [13] Z. Nibali, and D. Wollersheim, “Pulmonary nodule classification with deep residual networks”, International Journal of Computer Assisted Radiology and Surgery, vol. 12, pp. 1799-1808, 2017. <https://doi.org/10.1007/s11548-017-1605-6>
- [14] W. Shen, M. Zhou, F. Yang, D. Yu, D. Dong, C. Yang, Y. Zang, and J. Tian, “Multi-crop convolutional neural networks for lung nodule malignancy suspiciousness classification”, Pattern Recognition, vol. 61, pp. 663-673, 2017. <https://doi.org/10.1016/j.patcog.2016.05.029>
- [15] S. Hussein, K. Cao, Q. Song, and U. Bagci, “Risk Stratification of lung nodules using 3D CNN-based multi-task learning. Information Processing in Medical Imaging, vol. 10265, pp. 249-260, 2017. <https://doi.org/10.48550/arXiv.1704.08797>
- [16] Y. Xie , Y. Xia , J. Zhan, D. Feng , M. Fulham , and W. Cai, “Transferable multi-model ensemble for benign-malignant lung nodule classification on chest CT”, Lecture Notes in Computer Science, vol. 10435, pp. 656-664, 2017. <https://link.springer.com/chapter/10.1007/978-3-319-66179-775>
- [17] Y. Xie, Y. Xia, J. Zhang, M. Fulham, and Y. Zhang, “Fusing texture, shape, and deep model-learned information at the decision level for automated classification of lung nodules on chest CT”, Information Fusion, vol. 42, pp. 102-110, 2018. <https://doi.org/10.1016/j.inffus.2017.10.005>
- [18] Y. Xie , Y. Xia , J. Zhang, Y. Song, D. Feng, M. Fulham, and W. Cai, “Knowledge-based collaborative deep learning for benign-malignant lung nodule classification on chest CT”, IEEE Transactions on Medical Imaging, vol. 38, no. 4, pp. 991-1004, 2019. <https://doi.org/10.1109/TMI.2018.2876510>
- [19] G. Zhang, Z. Yang, L. Gong, S. Jiang, and L. Wang, “Classification of benign and malignant lung nodules from CT images based on hybrid features”, Physics in Medicine & Biology, vol. 64, no. 12, 2019. <https://doi.org/10.1088/1361-6560/ab2544>
- [20] P. Wu, X. Sun, Z. Zhao, H. Wang, S. Pan, and B. Schuller, “Classification of lung nodules based on deep residual networks and migration learning”, Computational Intelligence and Neuroscience, vol. 2020, pp. 1-10, 2020. <https://doi.org/10.1155/2020/8975078>
- [21] G. Shah, R. Thammajudjarit, A. Thakkinstian, and T. Suwatanapongched, “NoduleNet: a lung nodule



classification using deep learning”, Ramathibodi Medical Journal, vol. 43, no. 4, pp. 11-19, 2020
<https://doi.org/10.33165/rmj.2020.43.4.241727>

[22] E. Lv , W. Liu, P. Wen, and X. Kang, “Classification of benign and malignant lung nodules based on deep convolutional network feature extraction”, Journal of Healthcare Engineering, vol. 2021, no. 8769652, pp. 1-11, 2021. <https://doi.org/10.1155/2021/8769652>

[23] G. Zhang, L. Lin, and J. Wang , “Lung nodule classification in CT images using 3D densenet”, Journal of Physics: Conference Series, vol. 1827, pp. 1-7, 2021. <https://doi.org/10.1088/1742-6596/1827/1/012155>

[24] P. Bruntha , S. Pandian, J. Anitha, S. Abraham, and S. Kumar, “A novel hybridized feature extraction approach for lung nodule classification based on transfer learning technique”, Journal of Medical Physics, vol. 47, no. 1, pp. 1-9, 2022. https://doi.org/10.4103/jmp.jmp_61_21



Dr. Ahmed Nidhal Khdiar was born in Baghdad (Iraq), in 1982. Earn Ph.D. in electronic engineering- signal processing from USM University (Benign, Malaysia) in 2015. M.Sc. and B.Sc. in Electronic and Communication Engineering from Al-Nahrain University (Baghdad, Iraq) in 2004 and 2006 respectively).

He worked as an ENGINEER at *Iraqna* Company for Mobile

Phone Services. Also, Worked as an academic staff at Al-Sadik University, Islamic University, and Al-Nahrain University. Currently, he is a staff member of the University of Kufa, Najaf, Iraq.



Dr. Enas Hamood Al-Saadi obtained a computer science bachelor's degree, a master's degree, and a doctorate from Babylon University. She teaches as an associate professor at computer science- Babylon University. Her areas of interest in study are biomedical, computational intelligence, voice processing, image processing, and steganography. She has conducted numerous studies in the field of computer science.